Electronic Supplementary Material (ESI) for Physical Chemistry Chemical Physics.

Supporting Information

Can Duvelisib and Eganelisib Work for both Cancer and COVID-19? Molecular-level Insights from MD Simulations and Enhanced Samplings

Saroj Kumar Panda[a], Shaswata Karmakar[a], Parth Sarthi Sen Gupta[b], Malay Kumar Rana[a]*

[a]Department of Chemical Sciences, Indian Institute of Science Education and Research (IISER) Berhampur, Odisha-760010, India

[b]School of Biosciences and Bioengineering, D Y Patil International University, Akurdi, Pune

*Corresponding Author

Dr. Malay Kumar Rana,

Assistant Professor,

Department of Chemical Sciences,

Indian Institute of Science Education and Research (IISER) Berhampur,

Ganjam, Odisha, 760010, India

Email: mrana@iiserbpr.ac.in

Mobile: +91-680-2227753

Table S1: The electronic properties of Duvelisib and Eganelisib, derived using the DFT/B3LYP/6-311G+(d, p) level of theory.

Electronic properties (in eV)	**Eganelisib**	**Duvelisib**
HOMO	-0.2	-0.22
LUMO	-0.08	-0.06
Bandgap	0.12	0.16
Dipole moment (in Debye)	6.44	4.95
Ionization potential (IP)	0.2	0.22
Electron affinity (EA)	0.08	0.06
Electronegativity (χ)	0.14	0.14
Chemical potential (c)	-0.14	-0.14
Chemical hardness (η)	0.06	0.08
Chemical softness (σ)	16.85	12.13
Electrophilicity index (ω)	0.16	0.12

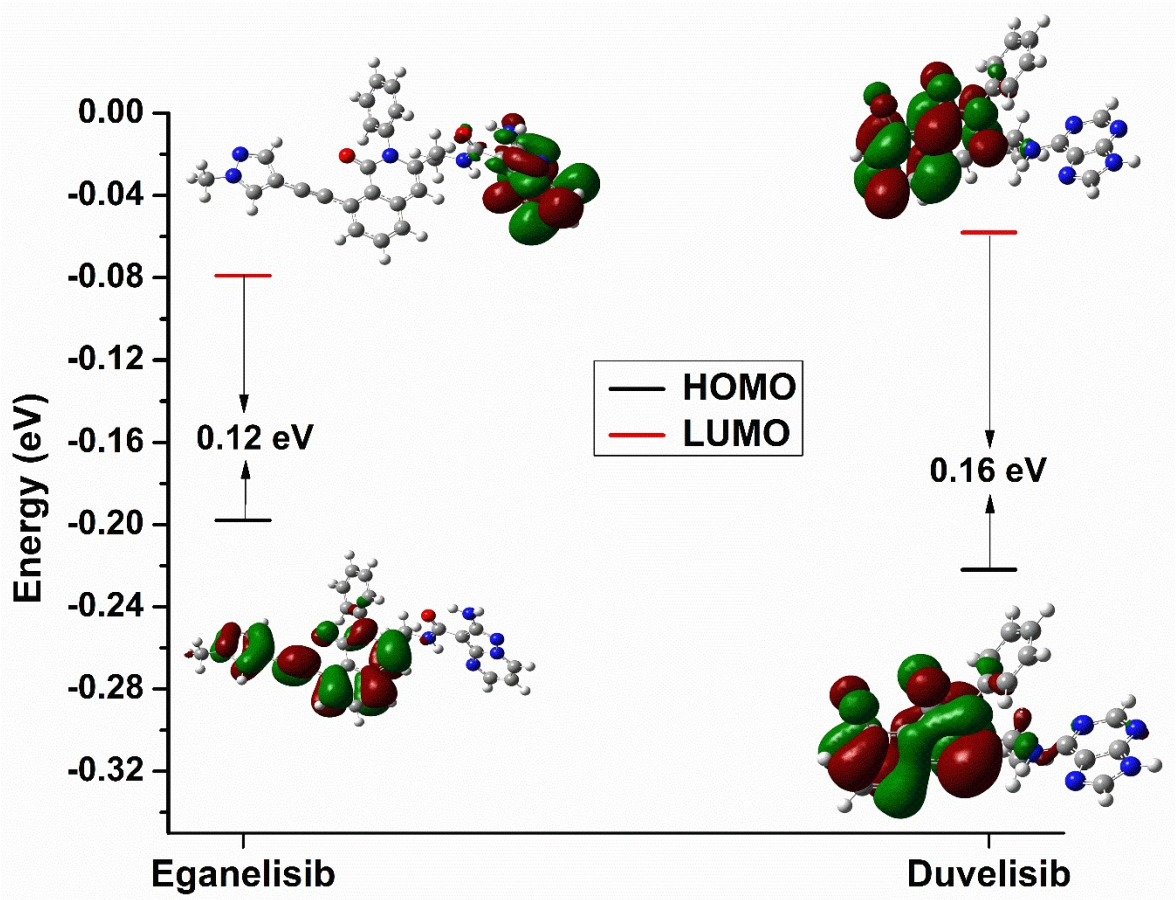

Figure S1: HOMO-LUMO energy levels and band gaps of Eganelisib and Duvelisib.

Table S2: The XYZ coordinates (in Å) of Duvelisib and Eganelisib before (initial) and after (final) DFT optimization of molecules at the BLYP/6-311G+(d,p) level of theory.

Duvelisib

Initial Coordinates			
C	0	0	0
C	0	0	1.53036
H	1.07926	0	1.87616
N	-0.66908	-1.21537	2.06825

C	0.01771	-2.36336	2.37534
C	-0.67231	-3.53326	2.83028
N	-2.02975	-3.83181	3.02031
C	-2.06584	-5.0916	3.46977
N	-0.75846	-5.66212	3.58935
C	0.13621	-4.67317	3.18009
N	1.50801	-4.71075	3.10053
C	2.05126	-3.55234	2.6457
N	1.39235	-2.40436	2.2803
C	-0.76258	1.20691	2.0853
C	-2.00903	1.52345	1.62518
C	-2.73902	2.65274	2.14075
C	-4.03959	2.95668	1.66354
C	-4.73063	4.04696	2.16416
C	-4.1541	4.8682	3.15273
C	-2.88261	4.57209	3.62087
Cl	-2.20906	5.59384	4.82662
C	-2.14564	3.46765	3.13412
C	-0.80196	3.16737	3.64707
O	-0.17261	3.78559	4.47585
N	-0.1616	1.985	3.08362
C	1.13942	1.60938	3.63405

C	2.27652	2.34547	3.27018
C	3.51503	1.98175	3.80592
C	3.6132	0.89981	4.68846
C	2.46879	0.17848	5.04727
C	1.22133	0.52989	4.52709
H	-0.99859	-0.13186	-0.43029
H	0.40736	0.93921	-0.39501
H	0.63102	-0.81651	-0.3825
H	-1.69181	-1.24049	2.06934
H	-2.95405	-5.65273	3.72534
H	-0.51382	-6.58605	3.90192
H	3.15162	-3.51836	2.55333
H	-2.47826	0.93328	0.84034
H	-4.4882	2.32353	0.89999
H	-5.73199	4.28056	1.798
H	-4.70583	5.72425	3.54038
H	2.19076	3.19962	2.59902
H	4.40605	2.54775	3.53719
H	4.58143	0.62198	5.10054
H	2.54841	-0.65993	5.73904
H	0.32699	-0.02533	4.80913
DFT-optimized Coordinates			

C	-0.83461	-1.68993	2.76297
C	-0.67992	-0.74258	1.55955
H	-1.02694	0.24509	1.8726
N	-1.56206	-1.1444	0.4459
C	-2.86509	-0.77221	0.35365
C	-3.67979	-1.15597	-0.73477
N	-3.42369	-1.92625	-1.87354
C	-4.57448	-1.93723	-2.53369
N	-5.56867	-1.21164	-1.88311
C	-5.00781	-0.70319	-0.7244
N	-5.57739	0.0673	0.22867
C	-4.71373	0.37383	1.21837
N	-3.41536	-0.00372	1.33023
C	0.74536	-0.63558	1.03038
C	1.63523	-1.66072	1.12332
C	2.9597	-1.57282	0.57189
C	3.8517	-2.66161	0.69071
C	5.12784	-2.58706	0.15607
C	5.54284	-1.42349	-0.51027
C	4.67401	-0.34572	-0.63252
Cl	5.35862	1.08642	-1.52467
C	3.364	-0.37901	-0.10094

C	2.41463	0.74617	-0.20249
O	2.65832	1.84109	-0.74775
N	1.12699	0.54545	0.37956
C	0.22461	1.68458	0.28853
C	0.22793	2.64807	1.30306
C	-0.63305	3.74639	1.2158
C	-1.48613	3.88314	0.11462
C	-1.4749	2.92165	-0.90231
C	-0.61661	1.82064	-0.81952
H	-0.62968	-2.73085	2.49255
H	-0.16384	-1.39902	3.57815
H	-1.86603	-1.62782	3.11982
H	-1.19824	-1.75938	-0.26904
H	-4.74963	-2.44141	-3.46955
H	-6.52036	-1.07101	-2.18205
H	-5.09766	0.98993	2.02144
H	1.35225	-2.57401	1.62849
H	3.52044	-3.55684	1.20684
H	5.81258	-3.42353	0.24755
H	6.53692	-1.35431	-0.93309
H	0.90601	2.53943	2.14272
H	-0.63294	4.49392	2.00205

H	-2.1531	4.73643	0.04747
H	-2.12922	3.02914	-1.76093
H	-0.59277	1.07514	-1.60575
<u>Eganelisib</u>			
Initial Coordinates			
C	0	0	0
C	0	0	1.52946
H	1.06863	0	1.90081
N	-0.63954	-1.23571	2.04323
C	-0.24948	-1.78047	3.26477
O	0.67994	-1.27824	3.9063
C	-0.96018	-2.96049	3.73464
C	-2.06772	-3.64769	3.21042
N	-2.85266	-3.49647	2.10434
C	-3.86136	-4.37108	1.92537
C	-4.14204	-5.43159	2.82201
C	-3.36096	-5.61044	3.95794
N	-2.32964	-4.72743	4.15566
N	-1.44755	-4.72963	5.21009
C	-0.59548	-3.65525	4.96188
N	0.46468	-3.33919	5.7566

C	-0.76197	1.23154	2.03891
C	-2.12372	1.29556	1.96799
C	-2.8543	2.44612	2.43326
C	-2.15001	3.55417	2.95354
C	-0.68311	3.53478	3.02292
O	0.04719	4.41793	3.42241
N	-0.03503	2.3194	2.54709
C	1.4218	2.26955	2.65012
C	2.19196	3.06257	1.78618
C	3.58421	3.02787	1.89649
C	4.1962	2.21427	2.85559
C	3.41669	1.43018	3.71278
C	2.02388	1.45349	3.62121
C	-2.88036	4.68912	3.41381
C	-4.27621	4.69618	3.34141
C	-4.96364	3.58664	2.81858
C	-4.27067	2.47551	2.37016
C	-2.22318	5.82399	3.94651
C	-1.66754	6.79869	4.40453
C	-0.98795	7.90118	4.92562
C	-1.52789	9.10727	5.41521
N	-0.43955	9.87276	5.81565

C	-0.48304	11.21971	6.39764
N	0.74506	9.23458	5.61274
C	0.43789	8.0249	5.06944
H	-1.01274	0.01263	-0.42332
H	0.52115	0.88608	-0.38731
H	0.51598	-0.88343	-0.39879
H	-1.43819	-1.60342	1.52699
H	-4.47569	-4.22229	1.0252
H	-4.97203	-6.10796	2.62217
H	-3.52468	-6.41088	4.69159
H	0.59587	-3.78948	6.64656
H	0.98789	-2.48181	5.5491
H	-2.69595	0.46379	1.56472
H	1.70889	3.71484	1.05907
H	4.19224	3.64558	1.23746
H	5.28119	2.19382	2.93768
H	3.89451	0.79818	4.46072
H	1.41293	0.82698	4.28019
H	-4.83389	5.5618	3.69141
H	-6.05315	3.61034	2.77126
H	-4.80348	1.6161	1.96763
H	-2.55258	9.41843	5.48568

H	-1.05179	11.2196	7.34487
H	0.54236	11.58077	6.61703
H	-0.95069	11.93501	5.69635
H	1.18155	7.28866	4.79757
DFT-optimized Coordinates			
C	2.03269	-1.13858	3.16836
C	1.84524	-1.08816	1.65139
H	1.68571	-2.13762	1.2612
N	3.06884	-0.56241	0.99871
C	3.41459	-0.96492	-0.28901
O	2.74248	-1.81609	-0.88139
C	4.59728	-0.36414	-0.88924
C	5.45679	0.64946	-0.4334
N	5.5267	1.40797	0.69894
C	6.51856	2.3146	0.7875
C	7.4846	2.51528	-0.22968
C	7.43916	1.75756	-1.39452
N	6.43351	0.82958	-1.50129
N	6.2133	-0.0116	-2.56535
C	5.0929	-0.75685	-2.20062
N	4.57121	-1.7518	-2.9709
C	0.64772	-0.1874	1.31631

C	0.73789	1.17102	1.42169
C	-0.37654	2.03147	1.11998
C	-1.60919	1.46177	0.72851
C	-1.75392	0.00377	0.6278
O	-2.75211	-0.61831	0.32793
N	-0.56536	-0.78086	0.93374
C	-0.68297	-2.23093	0.79582
C	-1.44106	-2.94375	1.73732
C	-1.56846	-4.32794	1.59469
C	-0.948	-4.98849	0.52936
C	-0.19747	-4.26513	-0.40425
C	-0.06116	-2.88075	-0.28156
C	-2.70849	2.32012	0.43049
C	-2.55757	3.70588	0.53119
C	-1.32559	4.25758	0.92359
C	-0.24764	3.4401	1.21539
C	-3.96328	1.80058	0.03118
C	-5.0398	1.36375	-0.31214
C	-6.26389	0.81895	-0.70415
C	-7.45702	1.49612	-1.02671
N	-8.37731	0.50611	-1.34968
C	-9.77334	0.70715	-1.75671

N	-7.84838	-0.74425	-1.25345
C	-6.55458	-0.58131	-0.85986
H	2.18042	-0.1451	3.60971
H	1.15065	-1.57914	3.65303
H	2.89877	-1.75579	3.44153
H	3.58048	0.17713	1.48083
H	6.54826	2.91052	1.71105
H	8.26471	3.26427	-0.10041
H	8.15563	1.86318	-2.21984
H	4.8918	-1.89916	-3.91293
H	3.69489	-2.19101	-2.66775
H	1.66894	1.64127	1.72938
H	-1.94358	-2.42132	2.54991
H	-2.16061	-4.89133	2.31439
H	-1.05346	-6.06647	0.42322
H	0.28385	-4.78021	-1.23484
H	0.54135	-2.31553	-1.00165
H	-3.39616	4.36083	0.30415
H	-1.22765	5.34163	0.99551
H	0.70556	3.86757	1.5165
H	-7.66384	2.54863	-1.03693
H	-9.82881	1.3041	-2.68469

H	-10.26521	-0.26828	-1.95026
H	-10.34292	1.22188	-0.9623
H	-5.87404	-1.40487	-0.69847

Table S3: The binding affinity for Duvelisib, PDB ID, and functions of different SARS-CoV-2 protein targets.

Targets	**AutodockVina Score (kcal/mol)**	**SwissDock Score (kcal/mol)**	**DockThor Score (kcal/mol)**	**PDB ID**	**Functions[1]**
Mpro	-8.2	-8.7	-8.2	6LU7[2]	Cleaves at various sites of the non-structural protein chain and makes them functional
PLpro	-7.1	-7.7	-7.8	7CMD[3]	Cleaves NSP1, NSP2, NSP3 from N-terminal region and make them functional
NSP3-AMP site	-7.8	-8.2	-8.1	7JME[4]	
RdRp complex	-7.1	-7.7	-7.4	7L1F[5]	Consists of mainly NSP12 along with NSP7 and NSP8 helps in replication and methylation
Helicase-ADP site	-7.8	-8.2	-7.4	6XEZ[6]	Helps in replication and transcription of virus
Helicase-NCB site	-8.2	-7.5	-7.8		
NSP14-ExoN	-7.6	-7.6	-7.6	7N0C[7]	It has 3′-5′ direction Exoribonuclease activity and N7-guanine methyltransferase activity
NSP14 - N7MTase	-7.6	-8.3	-7.7		
NSP15-endoribonuclease	-7.1	-7.5	-7.9	6WXC[8]	It has some endoribonuclease activity which involves Mn^{2+} ions
NSP16-GTA site	-7.7	-8.6	-7.4	6WVN[9]	Helps in transfer of methyl group to Cap-0 viral mRNAs
NSp16-MGP site	-7.5	-7.6	-7.7		
NSp16-SAM site	-8.1	-7.1	-7.4		
N protein	-7.9	-8.3	-7.8	7CR5[10]	RNA packaging, organization of viral genome, enhance

					transcription efficiency M, E, and S protein translocation.

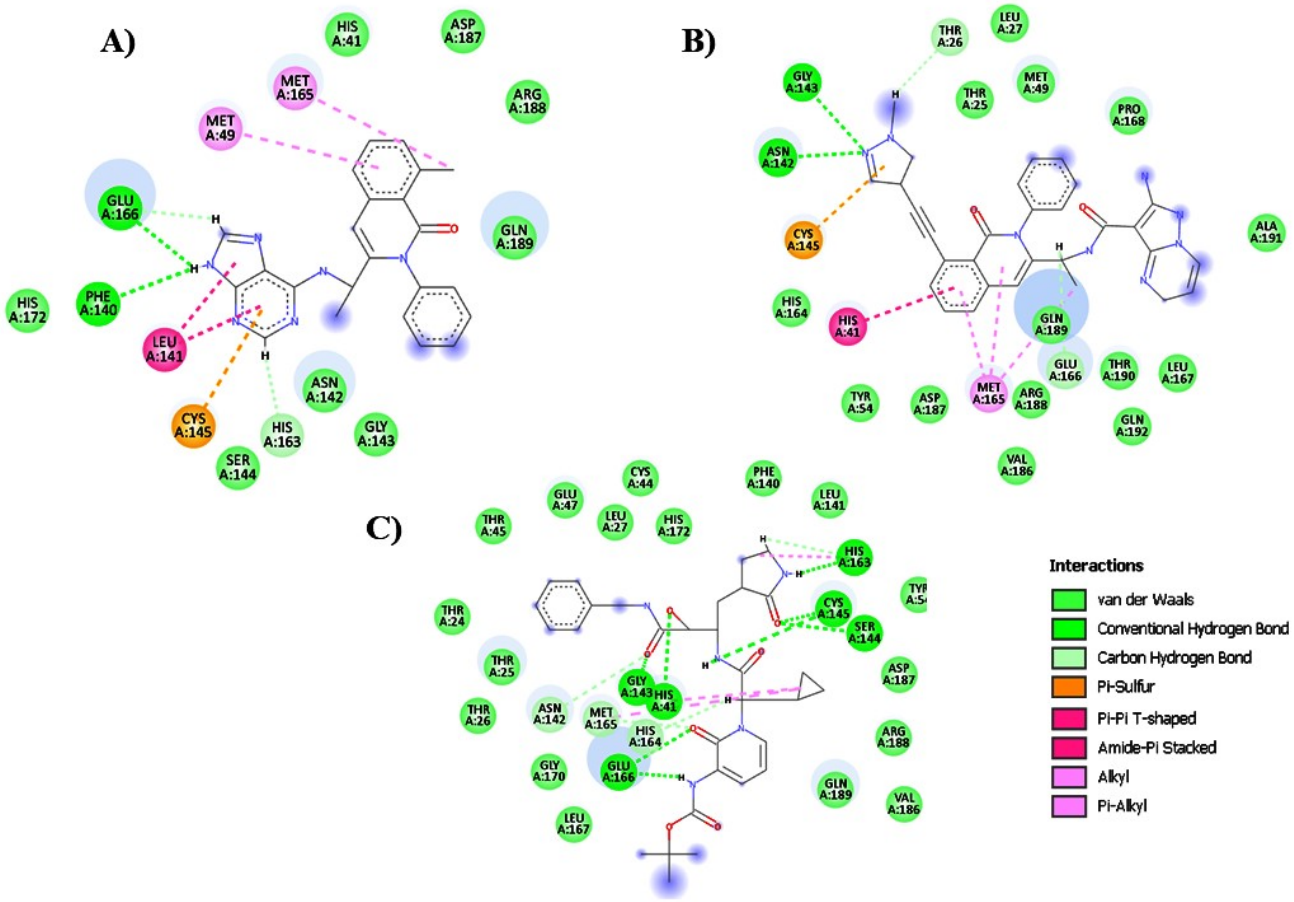

Figure S2: The 2D interaction plots before the MD simulation: (A) Mpro-Duvelisib, (B) Mpro-Eganelisib, and (C) Mpro-α-Ketoamide 13b.

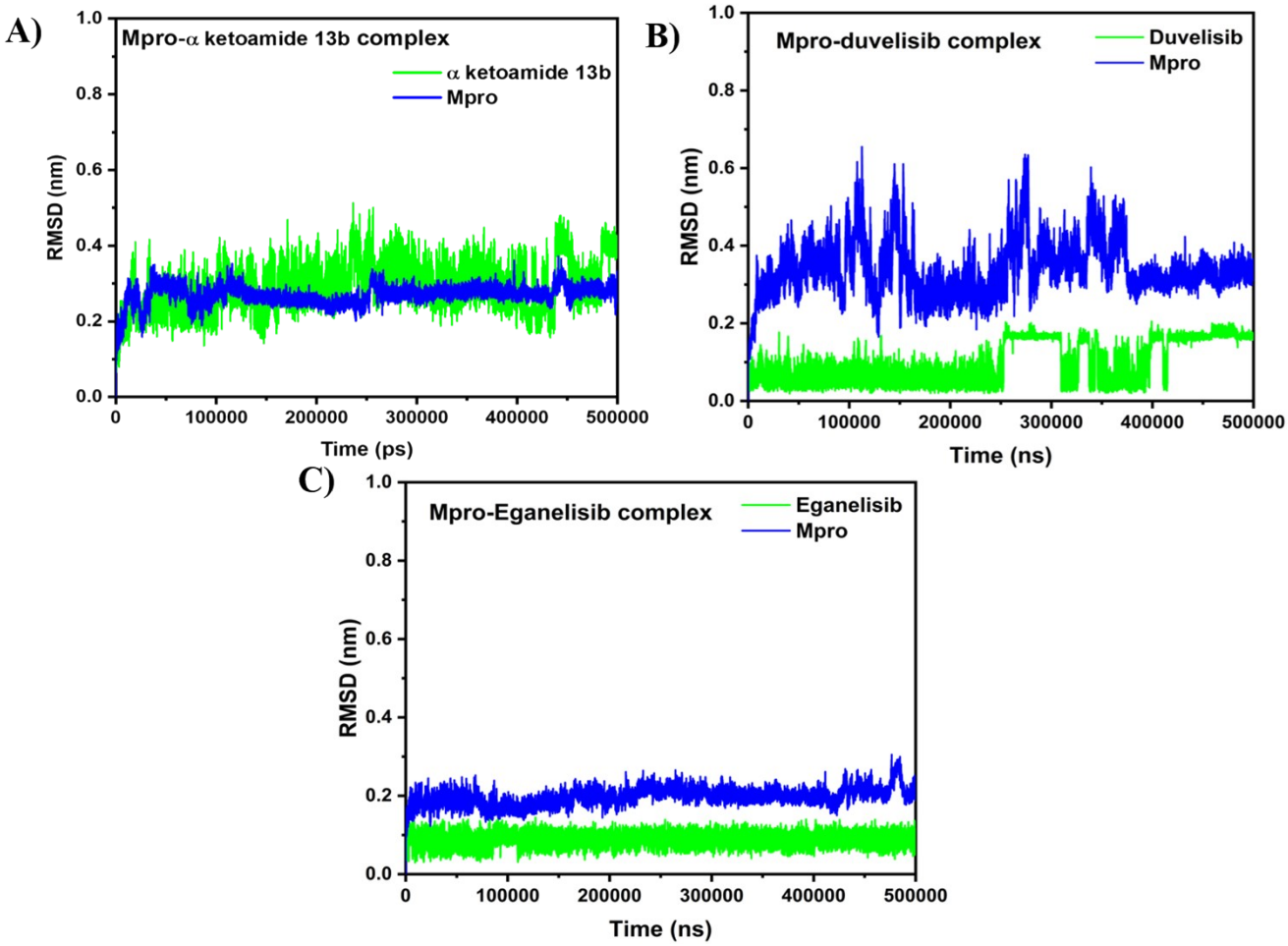

Figure S3: RMSD plots of the protein and ligand in the (A) Mpro-α-Ketoamide 13b, (B) Mpro-Duvelisib, and (C) Mpro-Eganelisib complexes.

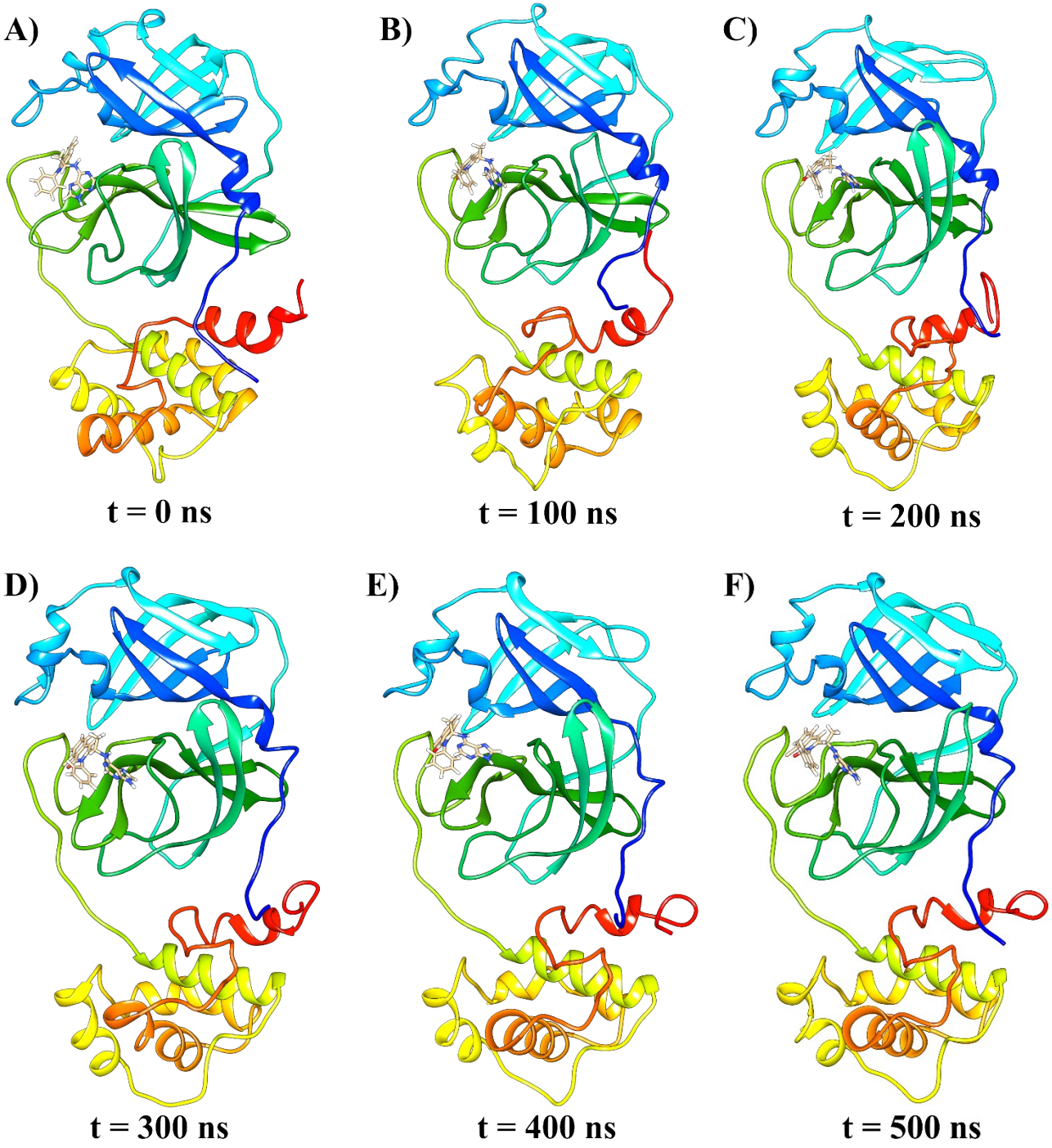

Figure S4: (A-F) MD snapshots of Mpro-Duvelisib taken at various times (t = 0-500 ns).

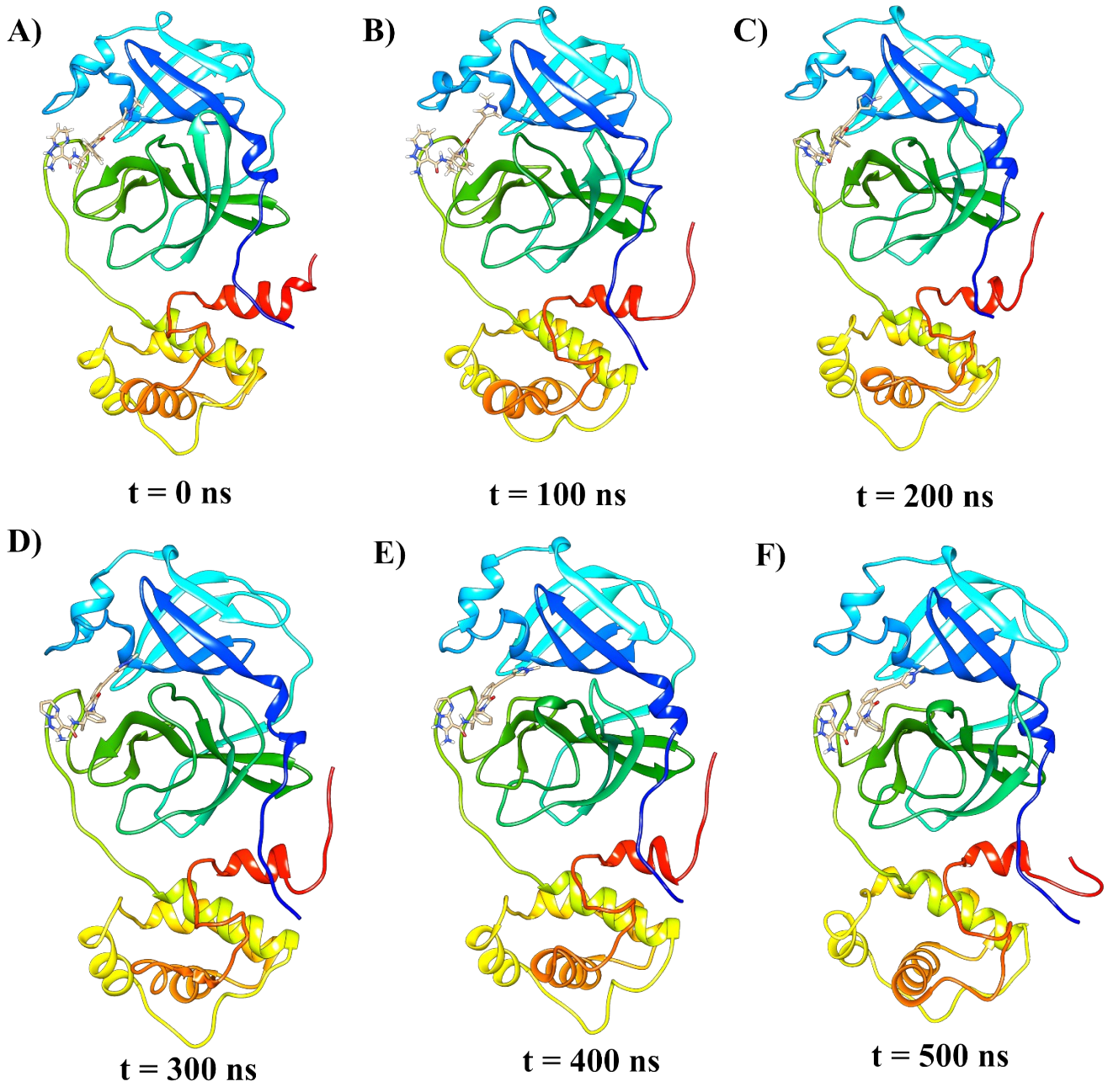

Figure S5: (A-F) MD snapshots of Mpro-Eganelisib at various time instants (t = 0-500 ns).

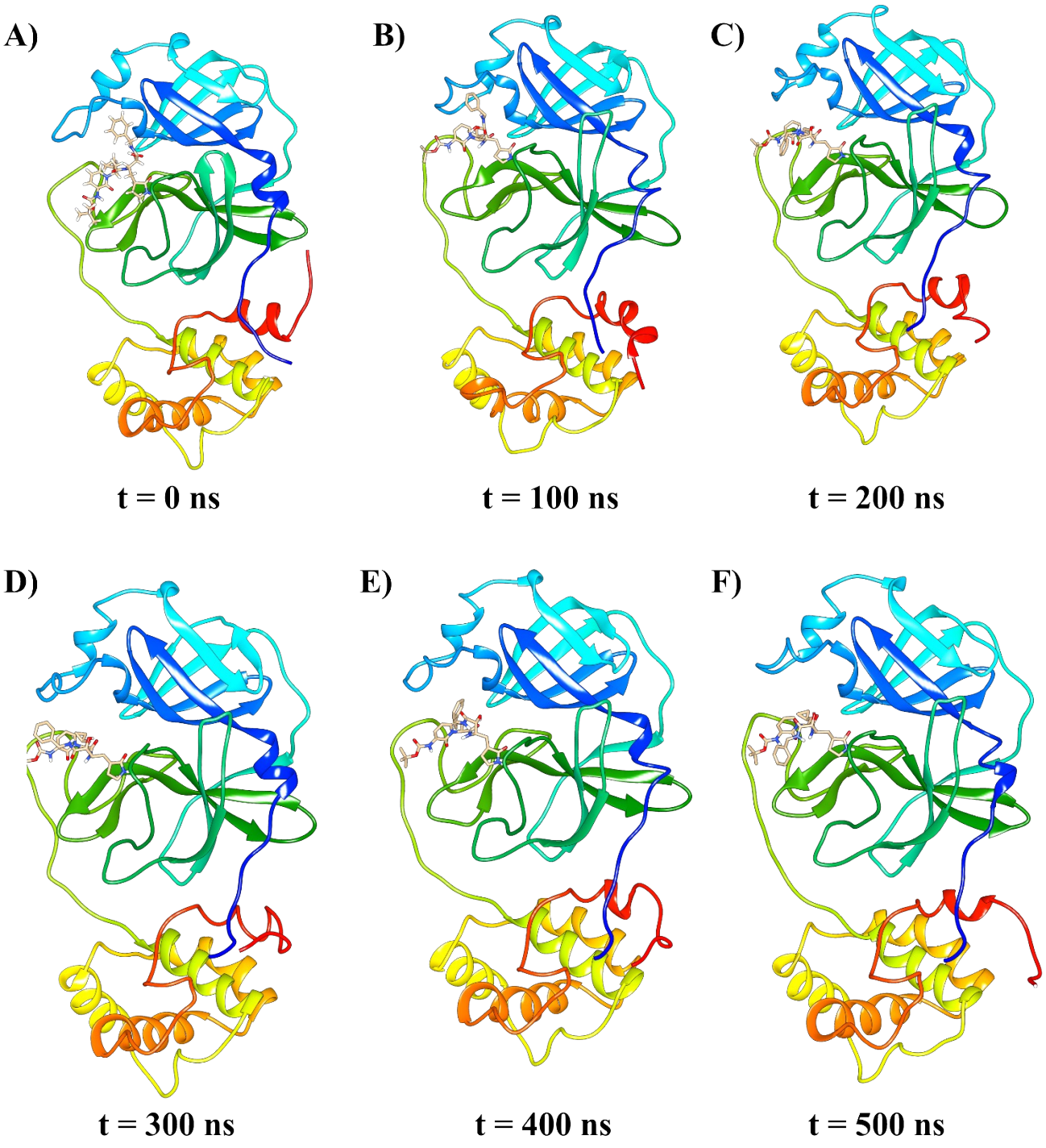

Figure S6: (A-F) MD snapshots of Mpro-α-Ketoamide 13b taken at various times (t = 0-500 ns).

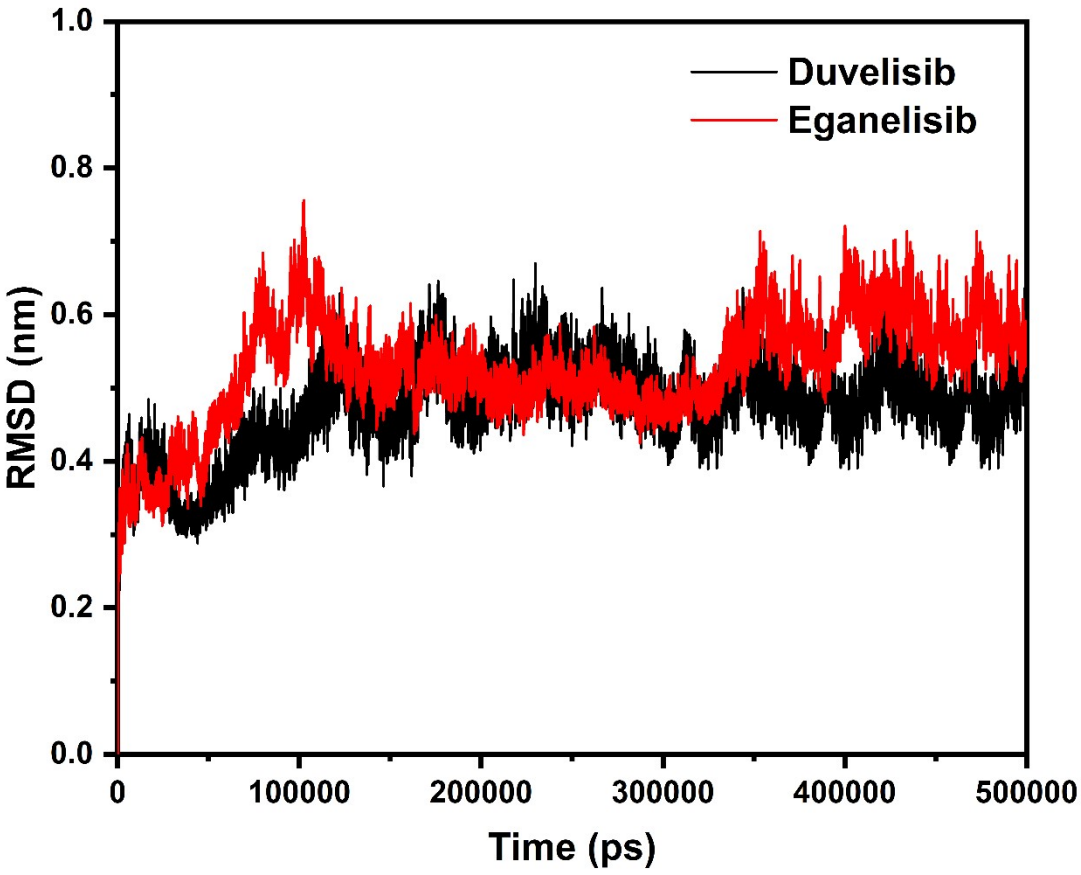

Figure S7: RMSD plots for Helicase NCB site-Duvelisib (black) and Helicase NCB site-Eganelisib (red).

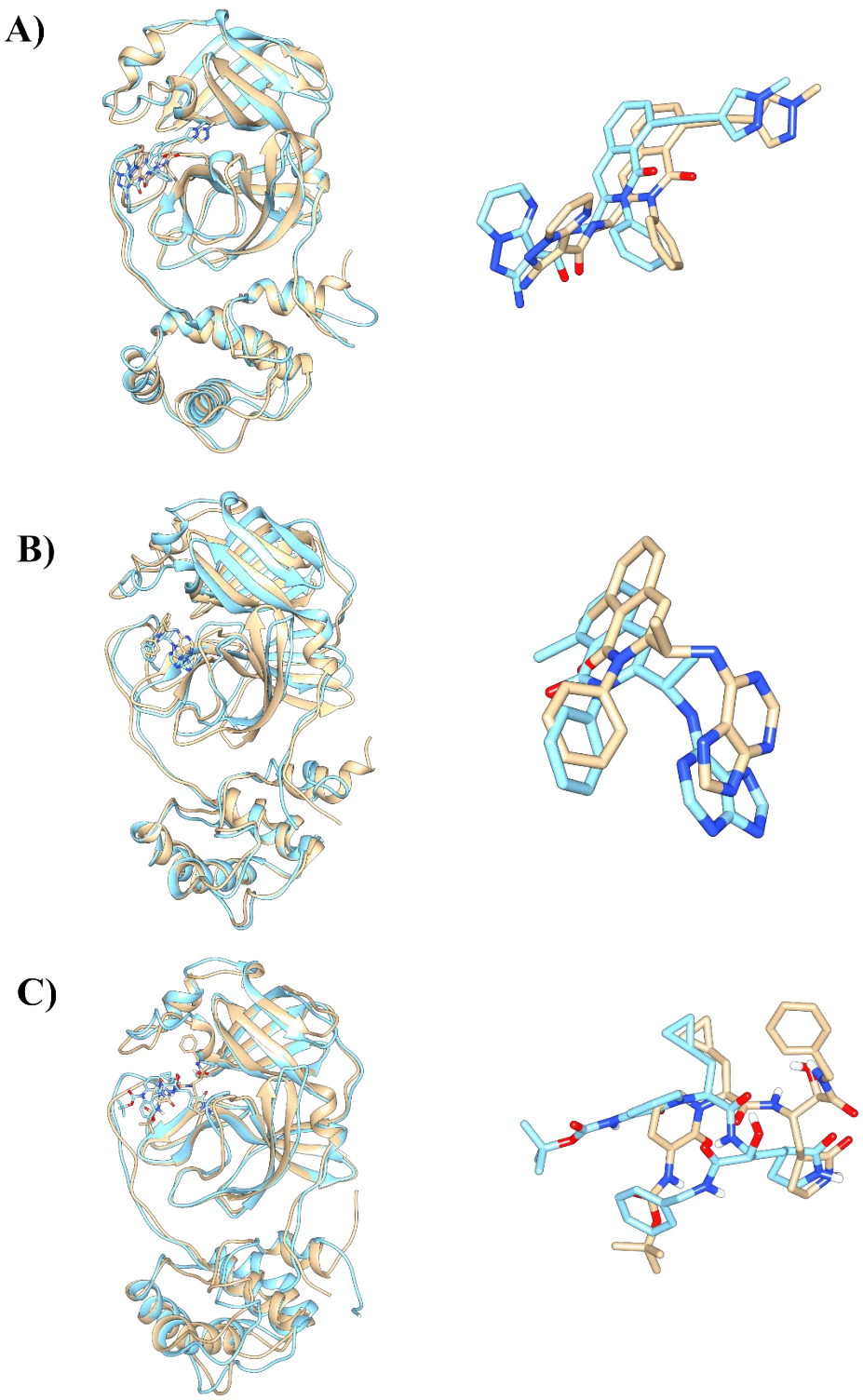

Figure S8: Displaying the superimposed structures of (A) Mpro-Eganelisib, (B) Mpro-Duvelisib, and (C) Mpro-α-Ketoamide 13b between 0 and 500 ns.

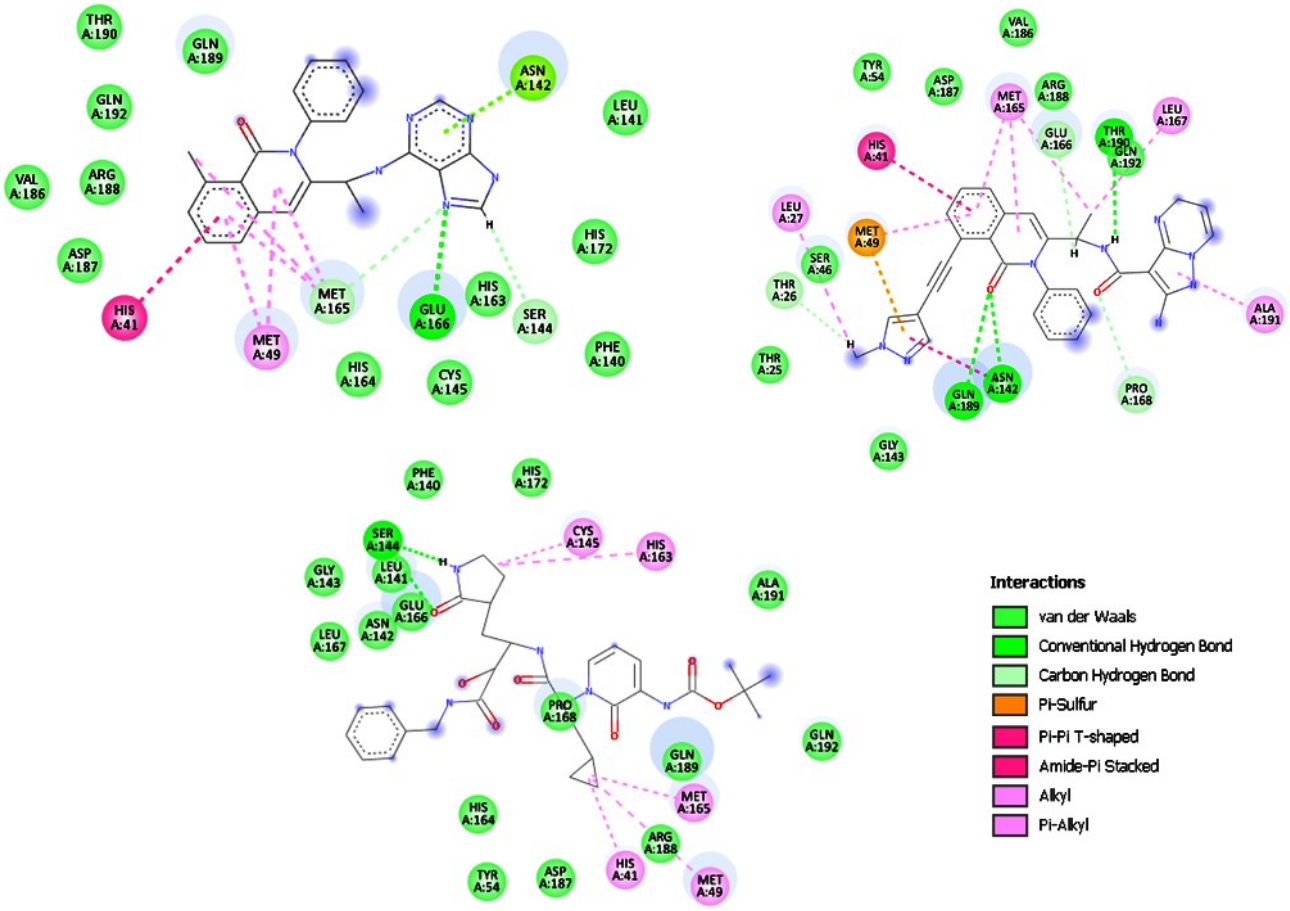

Figure S9: The 3D images captured at 500 ns display (A) Mpro-Duvelisib, (B) Mpro-Eganelisib, (C) Mpro-α-Ketoamide 13b interactions.

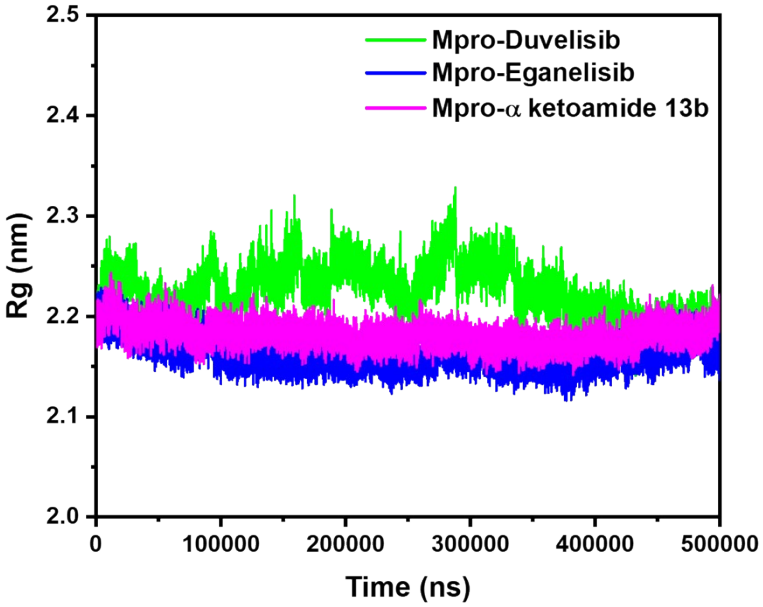

Figure S10: R_g plots for Mpro-Duvelisib (green), Mpro-Eganelisib (blue), and Mpro-α-Ketoamide 13b (magenta).

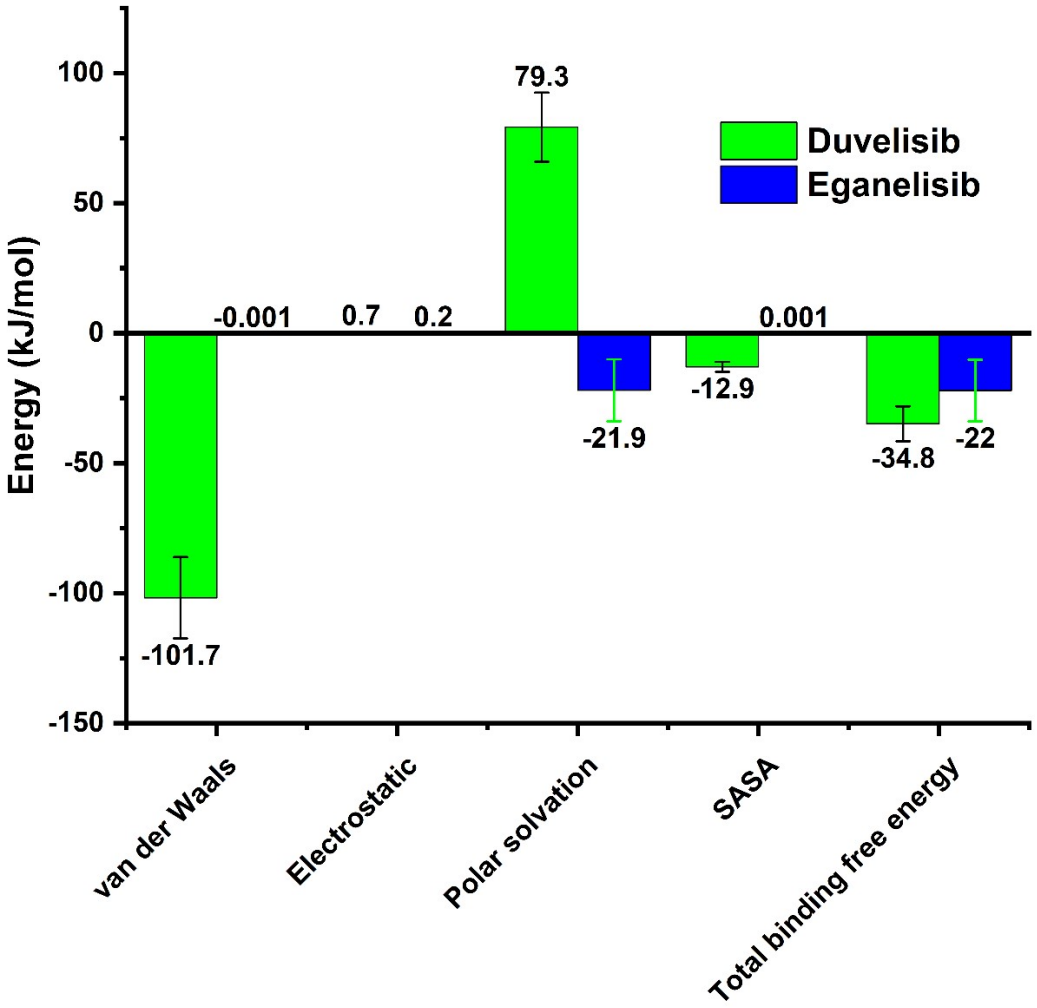

Figure S11: The total binding free energy and other contributing energies in kJ/mol for Helicase NCB site-Duvelisib and Helicase NCB site-Eganelisib.

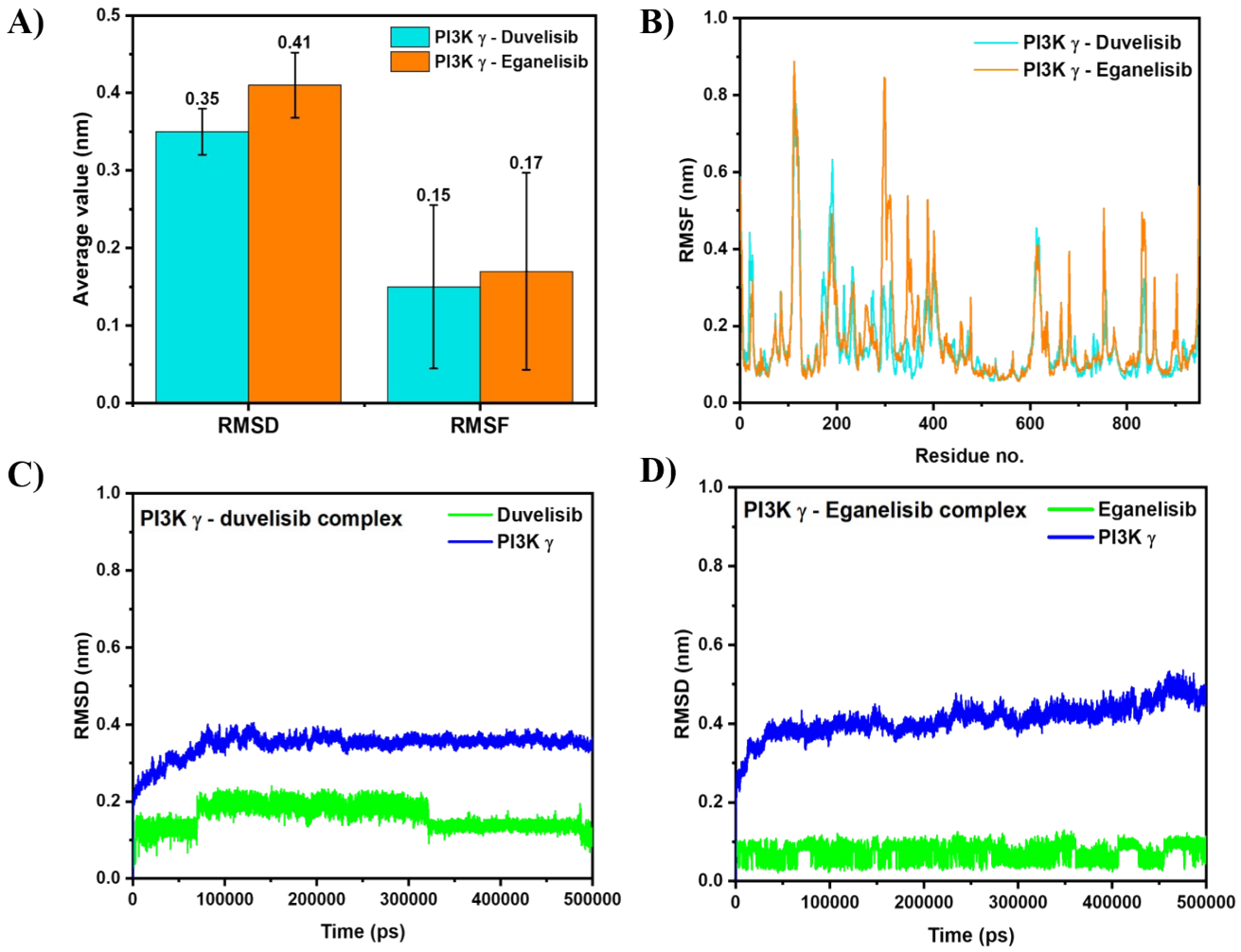

Figure S12: (A) The average RMSD and RMSF values of PI3Kγ-Duvelsib and PI3Kγ-Eganelsib and (B) the RMSF plots of PI3Kγ-Duvelsib and PI3Kγ-Eganelsib. The RMSD plots of protein and ligand of (C) PI3Kγ-Duvelsib and (D) PI3Kγ-Eganelsib.

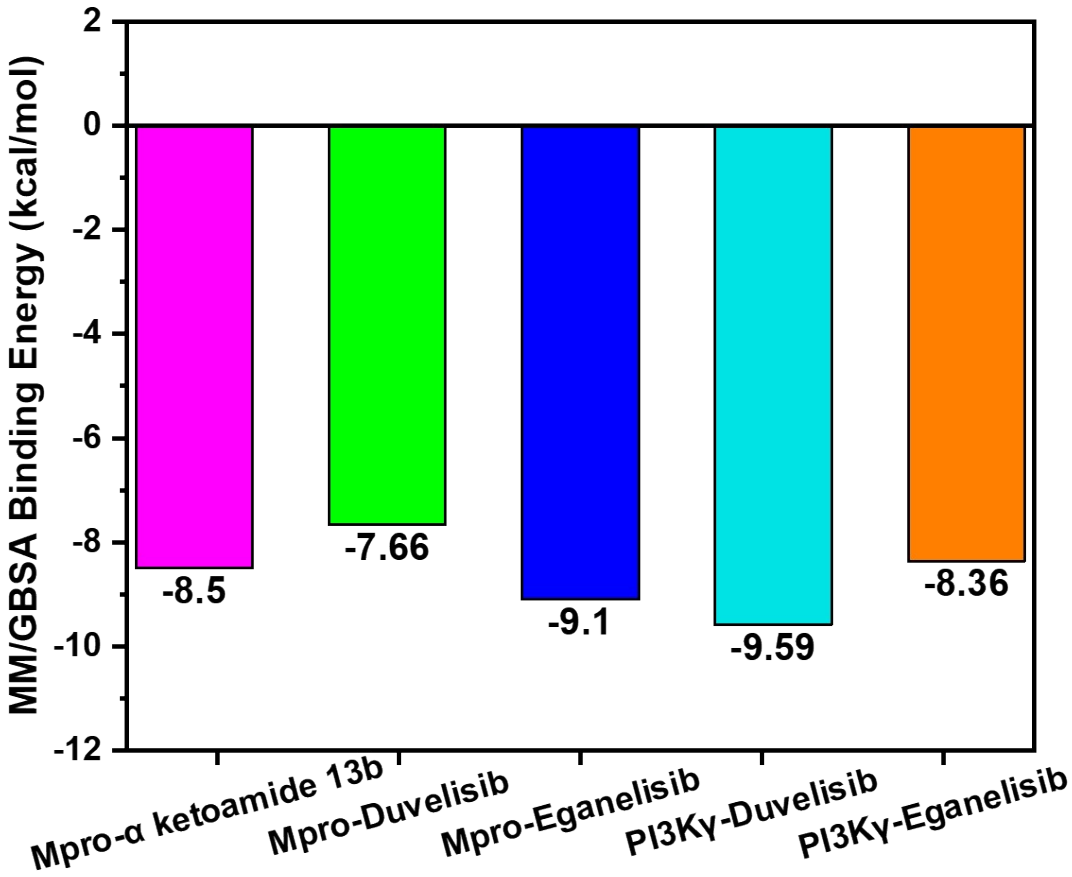

Figure S13: The MM-GBSA binding free energies (in kcal/mol) of Mpro-α Ketoamide 13b, Mpro-Duvelisib, Mpro-Eganelisib, PI3Kγ-Duvelsib, and PI3Kγ-Eganelsib.

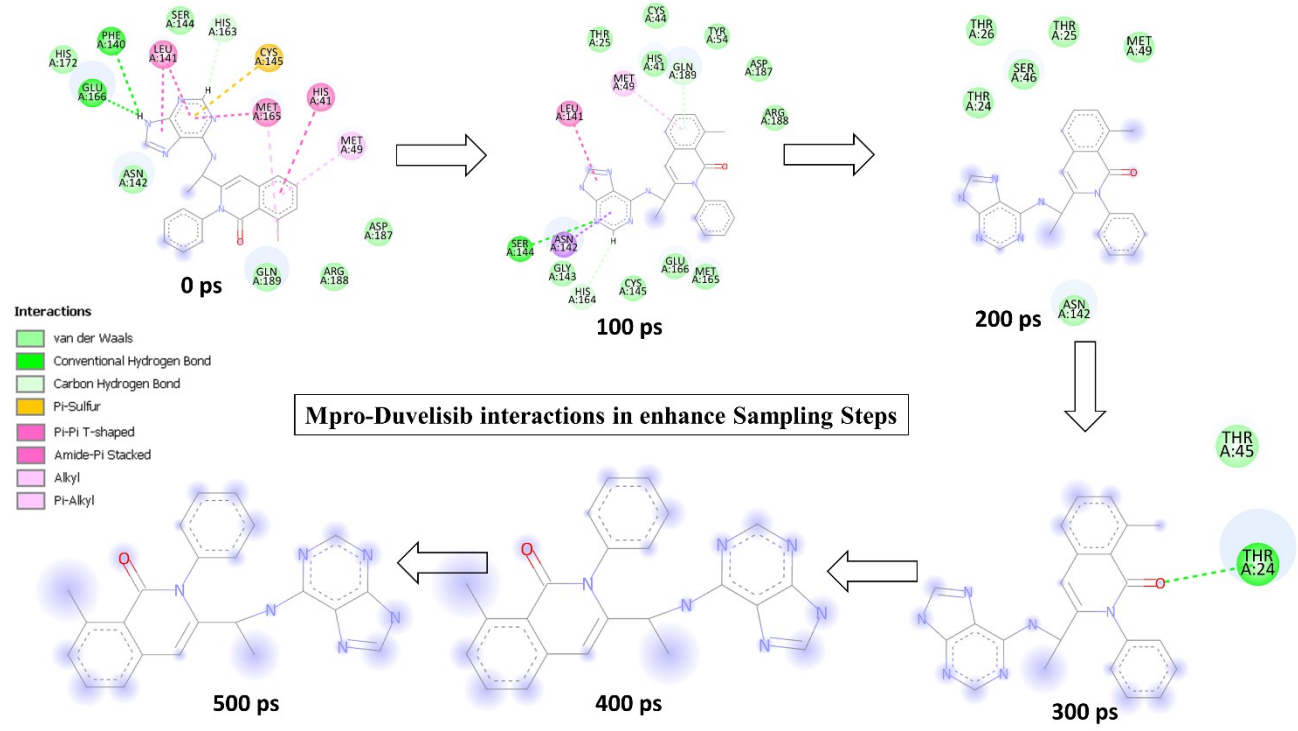

Figure S14: The 2D interaction snapshot of Mpro-Duvelisib in enhanced sampling steps.

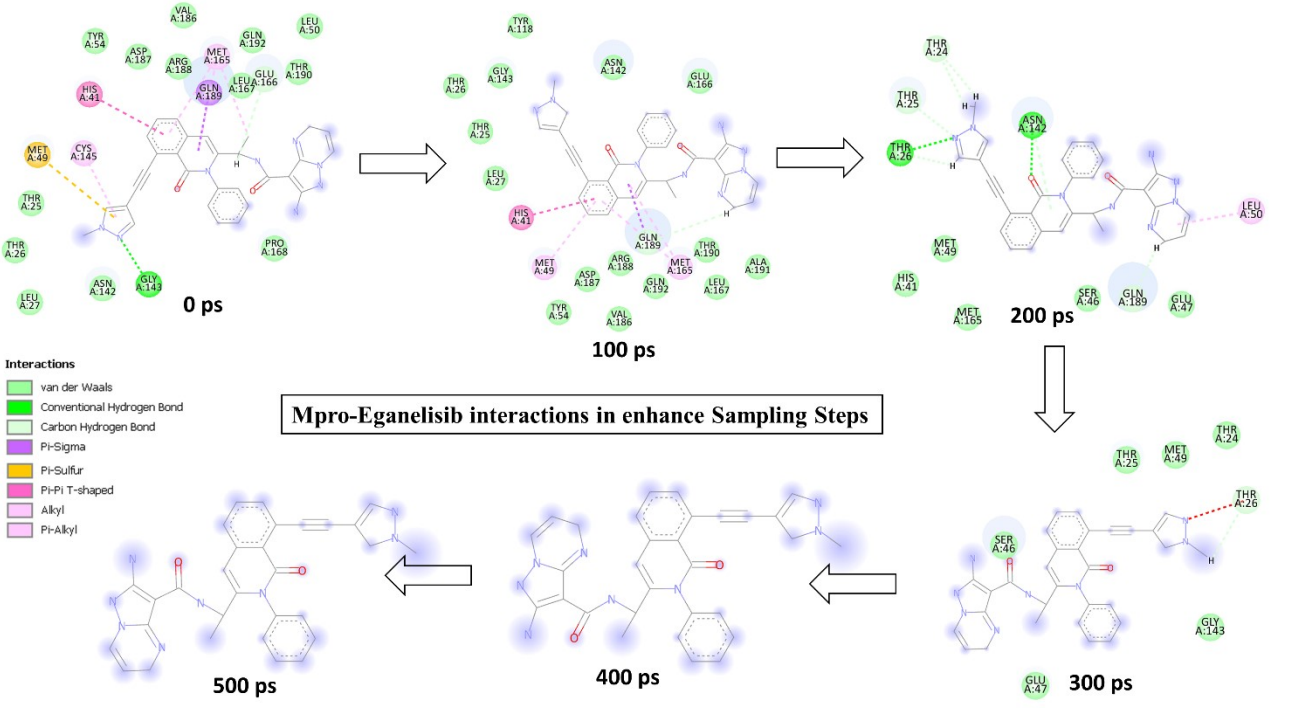

Figure S15: The 2D interaction snapshot of Mpro-Duvelisib in enhanced sampling steps.

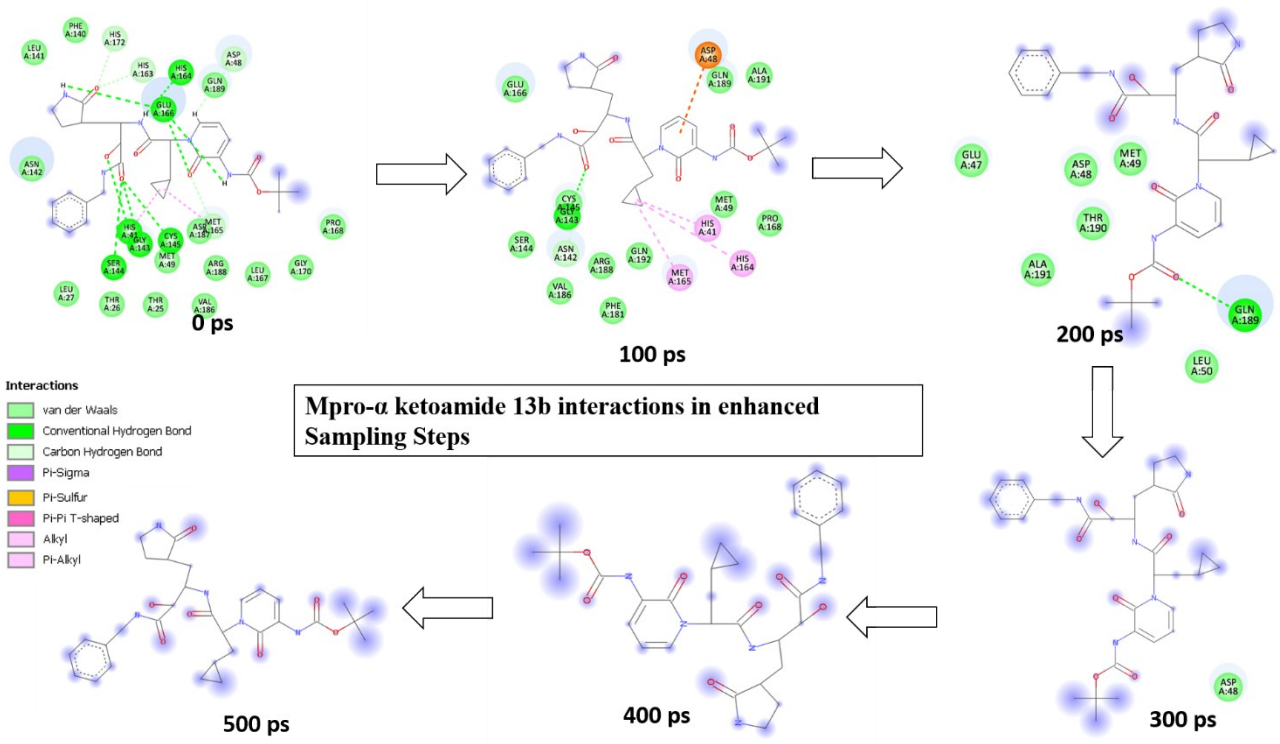

Figure S16: The 2D interaction snapshot of Mpro-α-Ketoamide 13b in enhanced sampling steps.

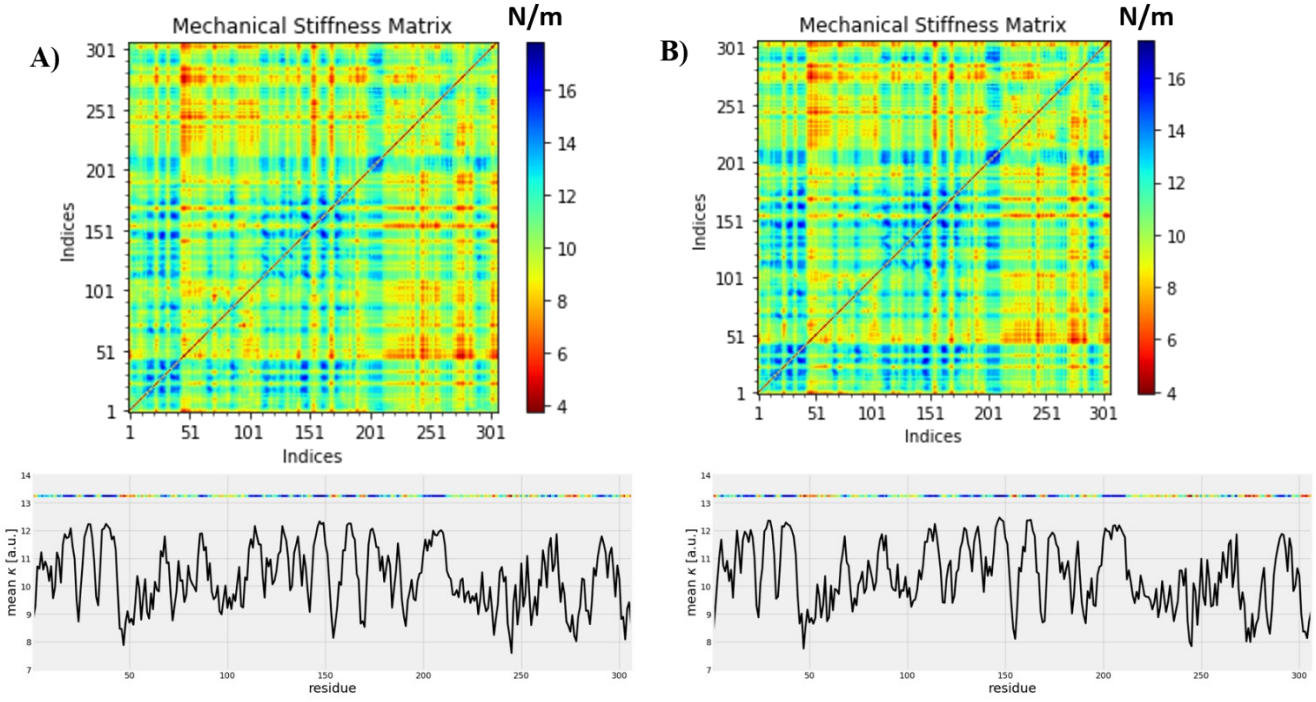

Figure S17: The mechanical stiffness maps for (A) Mpro-Duvelisib and (B) Mpro-Eganelisib, obtained by calculating the effective force constant in response to uniaxial external forces.

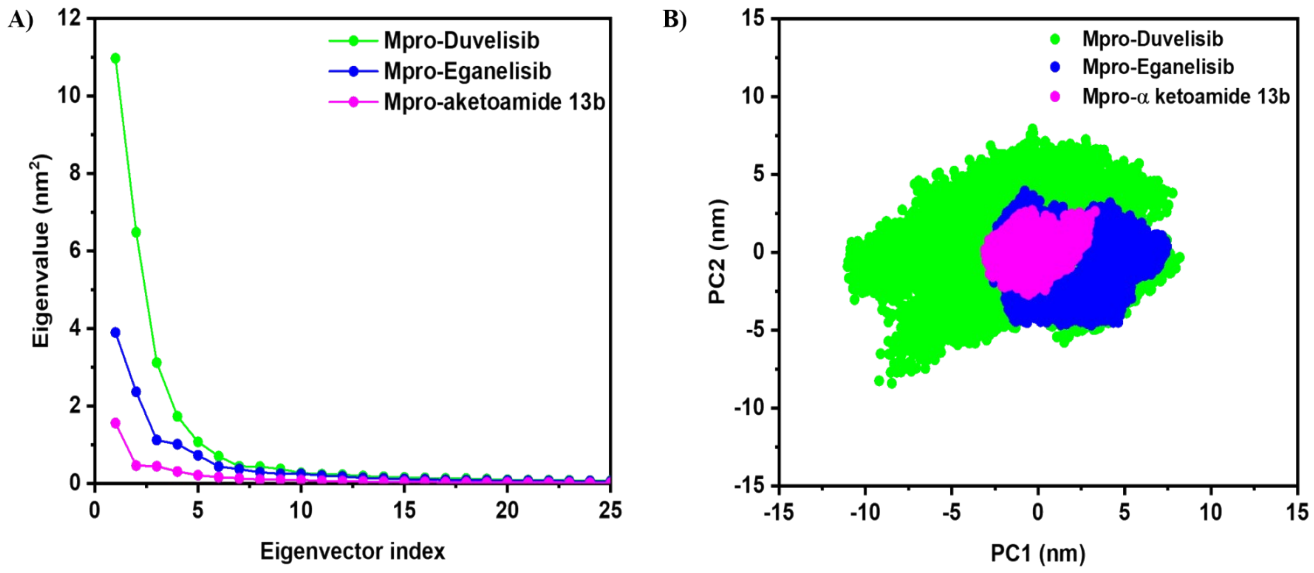

Figure S18: The principal component analysis (PCA) of Mpro-Duvelisib (green), Mpro-Eganelisib (blue), and Mpro-α-ketoamide 13b (magenta): (A) the plot of eigenvalues versus the corresponding eigenvector indices coming from the Cα covariance matrix during MD simulations and (B) the 2D projection plot of the first two principal eigenvectors.

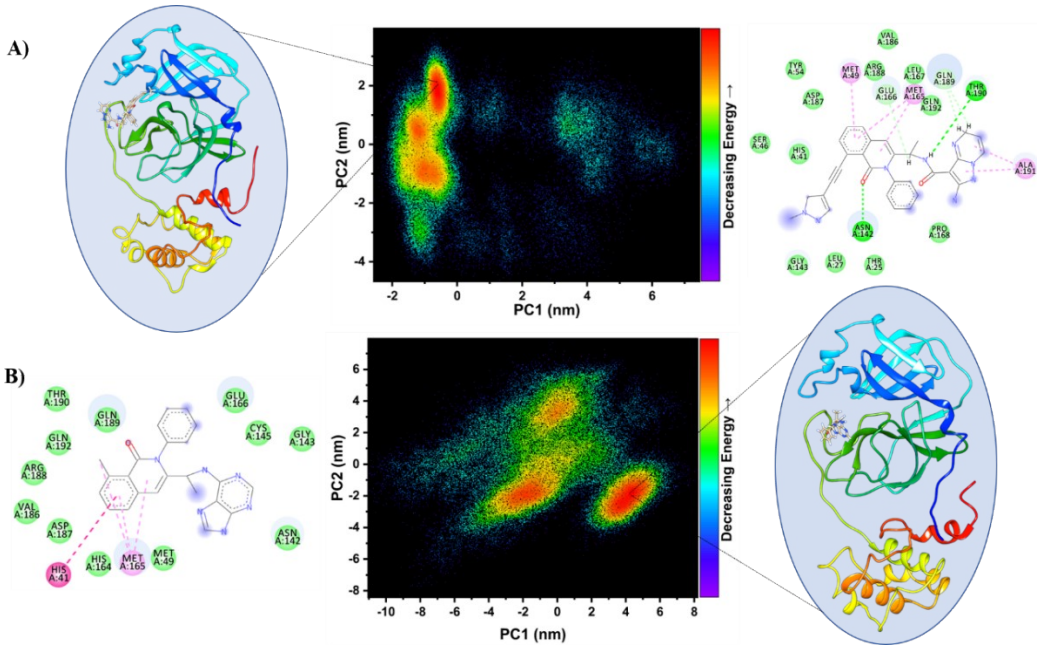

Figure S19: The Gibb's free energy landscape, lowest energy configuration, and corresponding 2D interaction plots for (A) Mpro-Eganelisib and (B) Mpro-Duvelisib.

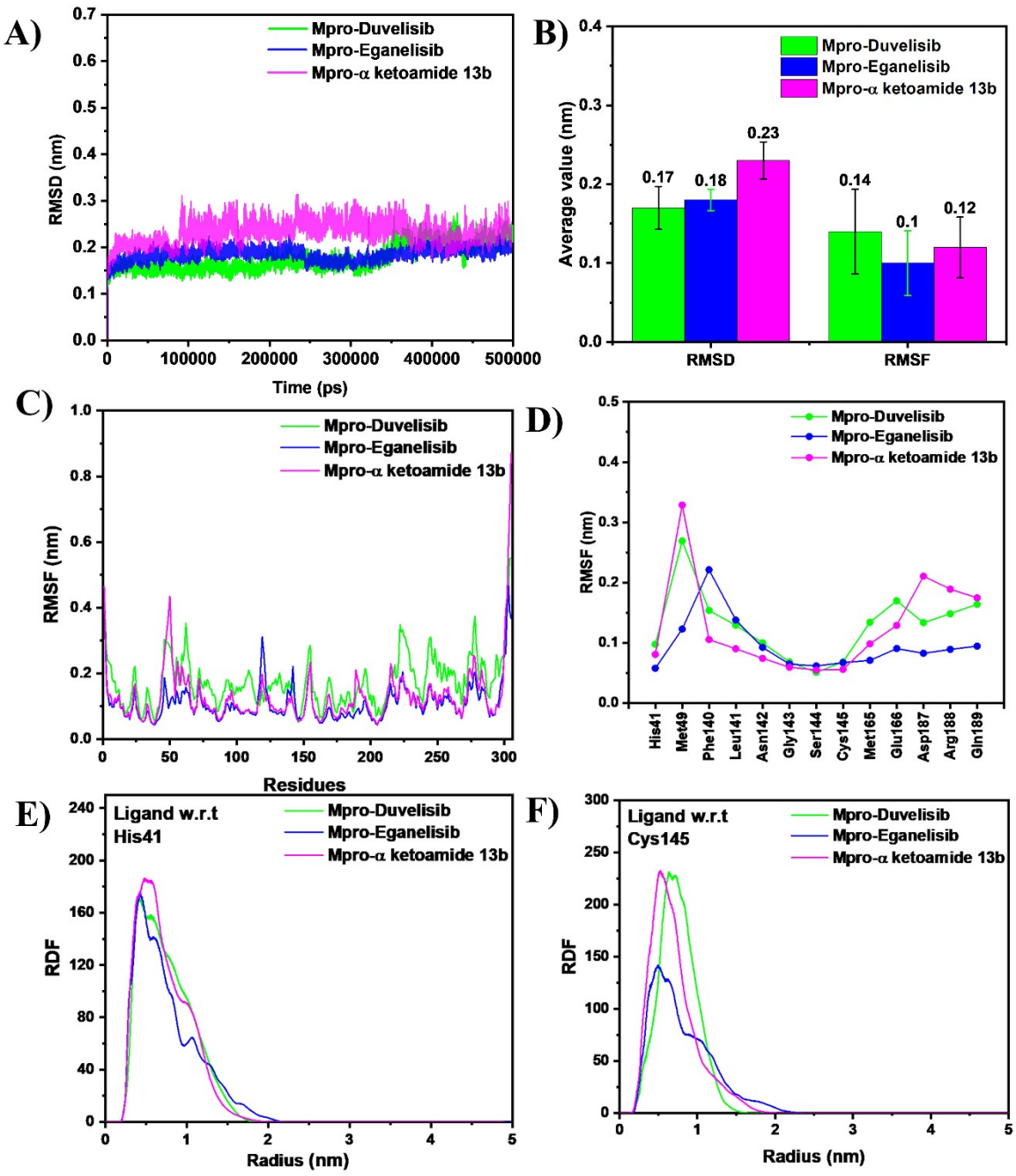

Figure S20: Illustrates AMBER99SB/TIP3P water model simulation results. (A) RMSD plots and (B) the average RMSD and RMSF values with standard deviations of Mpro's receptor binding domain (RBD) in the complexes of Duvelisib, Eganelisib, and α-Ketoamide 13b. (C) RMSF plots of the Cα-atoms of the Mpro-Duvelisib, Mpro-Eganelisib, and Mpro-α-Ketoamide 13b complexes, (D) RMSF plots of active site residues. (E) and (F) show radial distribution function (RDF) plots of the drug molecules with respect to His41 and Cys145 catalytic-dyad residues in the three complexes.

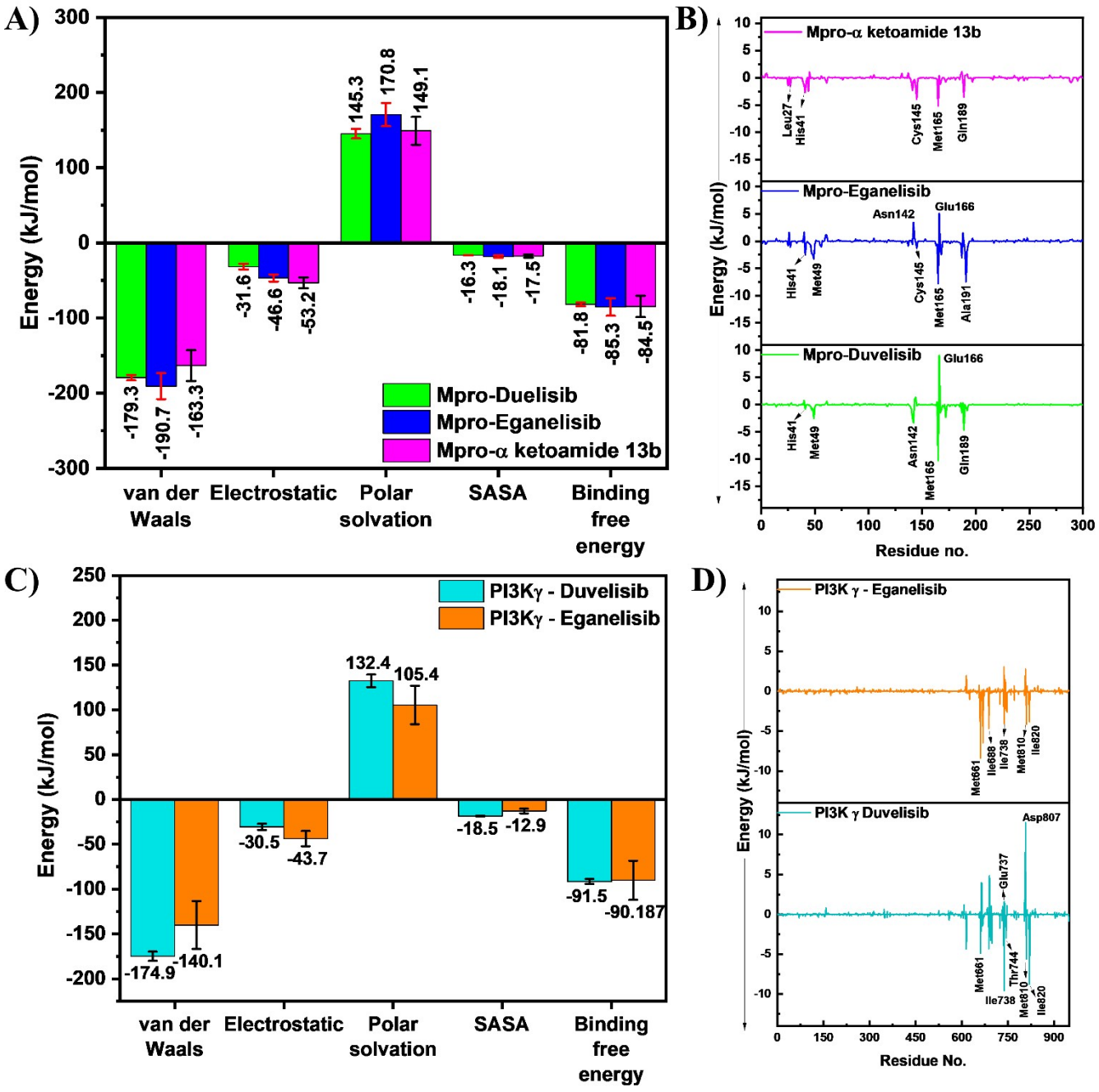

Figure S21: Illustrates AMBER99SB/TIP3P water model simulation results. The MM-PBSA binding free energy of Duvelisib, Eganelisib, and α-Ketoamide 13b with (A) Mpro and (C) PI3Kγ, including its various components. The per-residue energy contribution to the corresponding complexes of (B) Mpro and (D) PI3Kγ. All energies are in kJ/mol.

References

1. R. Yadav, J. K. Chaudhary, N. Jain, P. K. Chaudhary, S. Khanra, P. Dhamija, A. Sharma, A. Kumar and S. Handu, *Cells*, 2021, **10**.
2. Z. Jin, X. Du, Y. Xu, Y. Deng, M. Liu, Y. Zhao, B. Zhang, X. Li, L. Zhang, C. Peng, Y. Duan, J. Yu, L. Wang, K. Yang, F. Liu, R. Jiang, X. Yang, T. You, X. Liu, X. Yang, F. Bai, H. Liu, X. Liu, L. W. Guddat, W. Xu, G. Xiao, C. Qin, Z. Shi, H. Jiang, Z. Rao and H. Yang, *Nature*, 2020, **582**, 289-293.
3. X. Gao, B. Qin, P. Chen, K. Zhu, P. Hou, J. A. Wojdyla, M. Wang and S. Cui, *Acta Pharmaceutica Sinica B*, 2021, **11**, 237-245.
4. R. S. Virdi, R. V. Bavisotto, N. C. Hopper, N. Vuksanovic, T. R. Melkonian, N. R. Silvaggi and D. N. Frick, *SLAS Discovery*, 2020, **25**, 1162-1170.
5. J. P. K. Bravo, T. L. Dangerfield, D. W. Taylor and K. A. Johnson, *Molecular Cell*, 2021, **81**, 1548-1552.e1544.
6. J. Chen, B. Malone, E. Llewellyn, M. Grasso, P. M. M. Shelton, P. D. B. Olinares, K. Maruthi, E. T. Eng, H. Vatandaslar, B. T. Chait, T. M. Kapoor, S. A. Darst and E. A. Campbell, *Cell*, 2020, **182**, 1560-1573.e1513.
7. C. Liu, W. Shi, S. T. Becker, D. G. Schatz, B. Liu and Y. Yang, *Science*, 2021, **373**, 1142-1146.
8. Y. Kim, J. Wower, N. Maltseva, C. Chang, R. Jedrzejczak, M. Wilamowski, S. Kang, V. Nicolaescu, G. Randall, K. Michalska and A. Joachimiak, *Communications Biology*, 2021, **4**, 193.
9. M. Rosas-Lemus, G. Minasov, L. Shuvalova, N. L. Inniss, O. Kiryukhina, J. Brunzelle and K. J. F. Satchell, *Science Signaling*, 2020, **13**, eabe1202.
10. S. Kang, M. Yang, S. He, Y. Wang, X. Chen, Y.-Q. Chen, Z. Hong, J. Liu, G. Jiang, Q. Chen, Z. Zhou, Z. Zhou, Z. Huang, X. Huang, H. He, W. Zheng, H.-X. Liao, F. Xiao, H. Shan and S. Chen, *Nature Communications*, 2021, **12**, 2697.